4ICEGE Thessaloniki-GREECE 2007

4th International Conference on
Earthquake Geotechnical Engineering
June 25-28, 2007
Paper No. 1656

ASPECTS OF SURFACE TOPOGRAPHY AND SITE EFFECTS - EXPERIMENTAL AND NUMERICAL STUDIES AT AEGION, GREECE

Olga-Joan KTENIDOU [1], Dimitrios RAPTAKIS[2], Paschalis APOSTOLIDIS[3], Kyriazis PITILAKIS[4]

ABSTRACT

The aim of this paper is to study aspects of the effects of topographic relief and lateral discontinuities on strong ground motion using 2D numerical analysis as well as recordings from earthquakes and microtremor measurements. The site chosen for this study is Aegion, Greece, a highly seismic area marked by a characteristic morphology, with the Aegion Fault dividing the city into two levels. This site comprises a permanent downhole array (CORSSA: CORinth Soft Soil Array) operating since 2002, while its geometry, the surface geology and the soil parameters are relatively well constrained. A detailed 2D soil model crossing the fault and comprising both levels of the area was recently constructed, based on in situ surveys and laboratory geotechnical tests. This paper presents dynamic 2D numerical analysis of a typical cross-section performed on a detailed model, using synthetic pulses as well as actual recordings at basement level. Numerical results are compared to the instrumental data in order to check the performance of the model of this complex site. Then, parametric analyses are performed on variations of the original model so as to highlight the influence of the site's different features, namely the surface topography, the uphill soil deposits and the downhill complex layering which resembles a basin. Results are retrieved in the time domain, indicating complex wave fields in the vicinity of the crest and toe, the uphill effects being due to topography and uphill layering and the downhill effects owing to the basin structure.

Keywords: topographic and site effects, 2D numerical modelling, Aegion, CORSSA

INTRODUCTION

Local site conditions can influence the characteristics of strong ground motion in various ways, collectively referred to as site effects. The local geology at a site can modify the amplitude, frequency content and duration of seismic motion as it travels from bedrock to the ground surface. Site effects are related to the thickness and impedance contrast between soil layers, the surface topography as exhibited by the relief, as well as the 'subsurface topography' in terms of lateral discontinuities, faults, valley and basin edges, inclined soil layers or soil–bedrock interfaces. Whilst soil layer effects have been investigated fairly extensively, surface and subsurface topography effects present more complications, since they are tied to two-dimensional phenomena such as focusing and defocusing of seismic energy, diffraction and refraction of body waves, generation of surface waves and interference patterns leading to complex wave fields.

[1] PhD Candidate, Department of Civil Engineering, University of Thessaloniki, Greece, Email: ktenidou@civil.auth.gr
[2] Lecturer, Department of Civil Engineering, University of Thessaloniki, Greece, Email: raptakis@civil.auth.gr
[3] Dr Geologist, Department of Civil Engineering, University of Thessaloniki, Greece, Email: pasapostolidis@gmail.com
[4] Professor, Department of Civil Engineering, University of Thessaloniki, Greece, Email: kpitilak@civil.auth.gr

In this study a site is chosen which combines several of the aforementioned geomorphological features. It is modeled based on existing knowledge of the geometry and properties of the geological structures and the model sensitivity is checked with respect to the type of input motion and material damping. The numerical results are compared to data from earthquakes recorded and microtremors measured at various locations at the site. Parametric analyses are then performed on variations of the original model so as to highlight the influence of the site's different features, namely topography in conjunction with layering and basin effects from complex non-horizontal layering.

THE SITE UNDER STUDY AND THE MODEL USED

The Corinth Soft Soil Array (CORSSA) is the site used in this study. CORSSA was developed in the region of the Gulf of Corinth, Greece, a highly seismic area comprising many WNW-trending, north-dipping active normal faults (Figure 1a). The city of Aegion, near which the array is located, is traversed by the Aegion fault. With an escarpment of around 40m–100m, it divides the city into two levels (Figure 1b). The city has been struck by significant earthquakes in the past, the strongest recent one being that of June 15, 1995 (Ms=6.2). The peak ground acceleration recorded uphill was nearly 0.5g, one of the strongest recorded in Greece.

The chosen region is not only marked by its characteristic surface topography defined by the relief, but is also marked by a complex 'subsurface topography', meaning the local geological conditions downhill. On the one hand, there is strong lateral discontinuity present along the fault. On the other hand, a characteristic feature of the site is that the depth of deposits uphill is very shallow (roughly 20m) while the soft deposits downhill have a significant thickness (roughly 170m at CORSSA). Thus this site is suitable for studying topographic and complex site effects, given all the geological structures present.

CORSSA array lies at the lower part of the city, on the hanging wall, near the coast. The soil profile downhill consists of soft loose marine materials overlying stiffer soil formations. Beneath these lies a hard conglomerate, followed by even stiffer radiolarites and finally the limestone bedrock is encountered at a depth of several hundred meters. As shown in Figure 1c, CORSSA vertical array consists of a down-hole array of four broad-band 3D accelerometers lying at depths: -14m, -31m, -57m and -178m as well as a surface accelerometer. The deepest accelerometer lies within the stiff conglomerate, so as to be used as a reference station. All instruments above lie within softer soil layers.

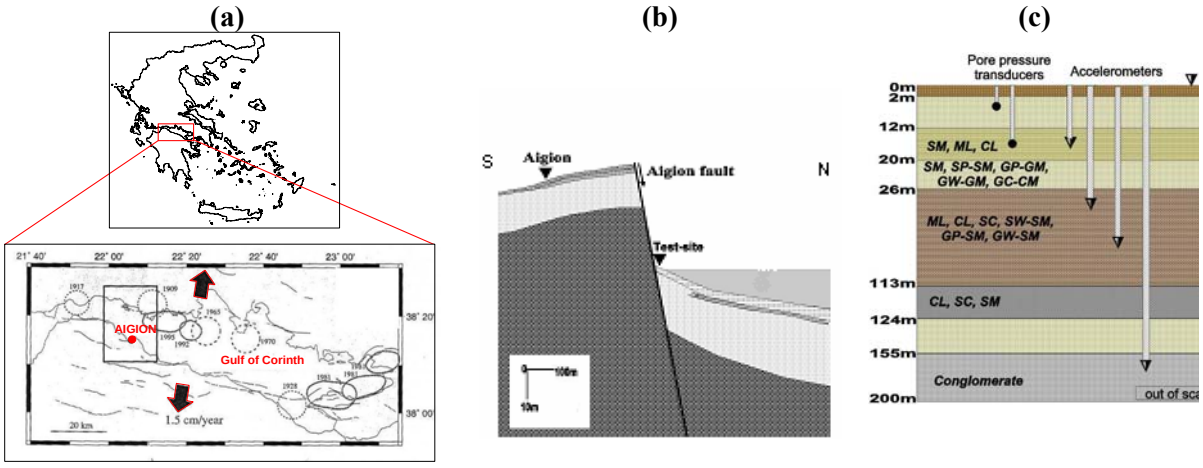

Figure 1. (a) Location of the Corinthian Gulf, Greece. (b) Sketch NS cross-section of Aegion city and fault. (c) Layout of the vertical CORSSA array.

After a series of field and laboratory tests and investigations, Apostolidis et al. (2005) finally modeled the complex geology of the site in sufficient detail and estimated the geotechnical and dynamic soil properties to a satisfactory degree. It was deduced that the soil layers as well as the conglomerate at the hanging wall are not horizontal, as had been the original assumption (Athanasopoulos, 1999; Pitilakis et al., 2004, 2004b & 2005), but actually dip towards the sea. The Aegion fault was found to be part of a complex geological structure which demonstrates a step-like morphology, the actual shear zone consisting of several incidental transitional faults. This contradicts the original assumption of a single normal fault dipping at a constant angle, constituting a single lateral discontinuity between the soft deposits downhill and the conglomerate uphill. The final model proposed can be seen in Figure 2.

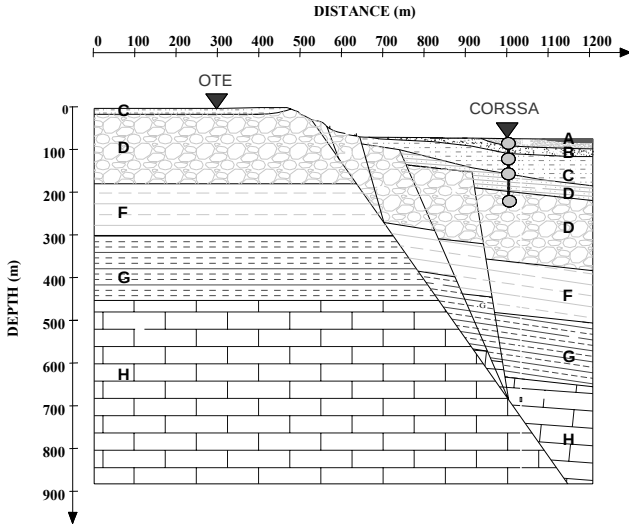

Formation	Description	Vs (m/sec)
A	Soft marine deposits consisting of sandy silt, silt, silt and clay (SM-ML-CL)	150-200
B	Soft sediments consisting of clayey silt, sandy clay, silty clay with few gravels (SC-ML-CL)	220-310
C	Hard deposits consisting of clayey silt, sandy clay, silty clay, with few gravels (SC-ML-CL)	370-490
D	Very hard deposits consisting of sandy gravels, sandy clay with few gravels (GW-GP-CL), NSPT	490-590
E	Stiff conglomerate with RQD 20% - 30%	800-1200
F	Marine clay	>800
G	Radiolarits and limestones	>1000
H	Limestone	>1200

Figure 2. Proposed geotechnical model for Aegion, along with the dynamic soil properties (after Apostolidis et al., 2005). Locations of surface and downhole accelerographs are also shown.

It is clearly seen that this structure is very complicated due to its various geological and geomorphological features. They are mentioned here along with some details on how the effects of such features are dealt with in geotechnical earthquake engineering. Firstly, it includes soil effects due to the horizontal soil deposit covering the conglomerate uphill. Such simple cases can be dealt with through 1D analysis as a matter of routine, as amplification is subject to impedance contrast. The site under study also includes topographic effects due to the relief, which complicate the matter. These have been studied over the past decades in various ways: experimentally (Chavez-Garcia et al., 1996, 1997), theoretically (Sanchez-Sesma and Campillo, 1993) and numerically (Assimakiet al., 2005; Bouckovalas and Papadimitriou, 2005). Detailed reviews can be found in Bard (1999) and Geli et al. (1988). Moreover, in this case, complex site effects are also expected due to the inclined deposits downhill as well as the inclined deposit-bedrock interface. These may bring to mind phenomena related to valley and basin-edge effects, such as soil resonance and lateral propagation of surface waves generated at the discontinuities. Such effects have been studied theoretically and experimentally by several researchers, such as Chavez-Garcia et al. (2000) and Raptakis et al. (2004).

MODEL SENSITIVITY CHECK

This process aims at comparing the results achieved through the particular numerical code used with available instrumental data from earthquakes and microtremor measurements. The sensitivity of the model is also investigated with respect to the kind of input motion used and the effect of damping. It also brings out the complexity of the response and the need to look into the different parameters in more detail.

Numerical modelling and analysis

The numerical analyses presented were performed with the finite difference code *FLAC 2D* (Itasca Consultants, 2002). An elaborate geotechnical model was implemented, reaching as far down as the conglomerate and accounting for the dipping layers at the hanging wall. The geometry and soil parameters attributed to the model are shown in Figure 3. The discretization allows for a maximum frequency of at least 10Hz to propagate through the finite difference grid without distortion. Rayleigh damping is used, centered around a certain frequency which ensures a quasi-equal mass and stiffness contribution. The lateral boundaries simulate free-field conditions, while the base through which the input motion is inserted is elastic (since the conglomerate is not the actual seismic bedrock – the underlying limestone is).

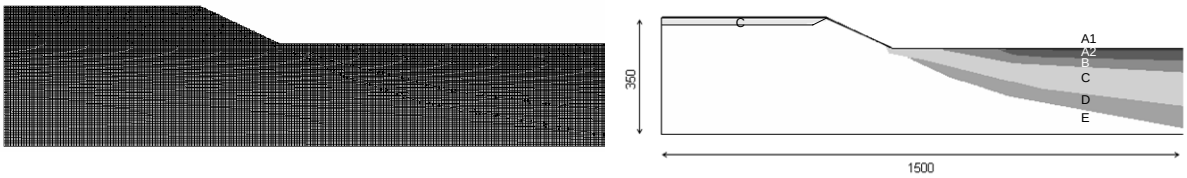

Figure 3. Soil model and finite difference grid used for 2D analysis.

The input motion consists of SV waves vertically propagating from the base. The input motions used comprise of: 1. A Gabor wavelet, which excites a broad band of frequencies up to 8Hz, thus replacing use of consecutive Ricker pulses, often used in such studies. 2. An earthquake recorded at all five stations of the CORSSA array (18/11/2003, 18:32:11.000, 38.410°N, 22.000°E, h=13km, ML=4.1, Re=19km).

The level of excitation assumed was of the order of 0.5g, bearing in mind the region's high seismicity and the 1995 event which caused similar PGA values to be recorded in the vicinity. Though it's not our objective here to investigate non-linearity, however, in order to account for larger strains in the 2D analysis at this high level of input, a 1D equivalent linear analysis was first carried out for the soil profile at CORSSA, using EERA code (Bardet et al., 2000), so as to estimate the strain compatible soil properties of each soil layer. The G-γ-D curves used to describe stiffness degradation and damping increase were derived from laboratory data made available through the CORSEIS Project (CORSEIS, 2000; Pitilakis et al., 2004). The curves corresponding to the soil layers as defined by Apostolidis et al. (2005) are seen in Figure 4. The conglomerate rock (soil type E) is considered as basement, having a Vs of the order of 1000m/s. The values of shear wave velocity (Vs), shear modulus (G) and damping (D) are shown in Table 1, for the small-strain case (indicated by the subscript '0') as well as the large-strain case of 0.5g. These new values calculated were then used as soil parameters for the 2D analyses that followed.

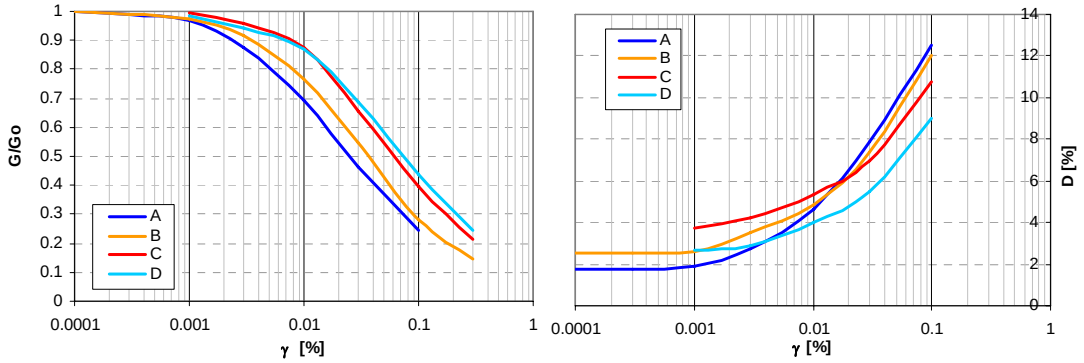

Figure 4. G-γ-D curves for all soil types used for the preliminary equivalent-linear 1D analysis.

Table 1. Physical, mechanical and dynamic properties for all soil layers of the 2D model (small-

strain and high-strain values depending on level of input).

Soil Type	γ [kg/m³]	ν (Poisson)	Small strain			0.5g input level			
			Go [MPa]	Vso [m/s]	Do [%]	G/Go	G [Mpa]	Vs [m/s]	D [%]
E	2100	0.20	2141	1010	0.5	1	2141	1010	0.5
D	2000	0.30	594	545	2.0	0.5	297	385	4.5
C	1950	0.30	385	444	2.7	0.9	347	422	6.0
B	1950	0.30	140	268	2.5	0.3	42	147	11.5
A(2)	1850	0.30	61	182	1.8	0.2	12	81	14.0
A(1)	1850	0.30	61	182	1.8	0.7	43	152	6.0

Instrumental data used

The numerical results were compared to data derived from earthquake recordings and noise measurements in order to check the numerical model.

Downhole array

From all the events recorded since the array began to operate, eight events were chosen (see Table 2), which correspond to earthquakes with M>4, based on extensive cross-checking with earthquake catalogues (National Observatory of Athens). The standard spectral ratios (SSR) were estimated for the recordings at the four upper stations (depths 0m, 14m, 31m, 57m) using the deepest station (depth 178m, in conglomerate) as a reference station (Figure 5d). The numerical results at the corresponding points in the model were used to estimate corresponding transfer functions. This was done for the damped model (0.5g strain level) using both a Gabor wavelet and the recording as input, with identical results (Figures 5a, b). This successfully allows us to use the synthetic wavelet for all future analyses, since it has much fewer requirements concerning time and computing memory. Ratios were also produced for the undamped model (Figure 5c). Compared to the empirical SSR, the analysis results successfully follow the peak shape (i.e., fundamental peak at 1Hz and higher modes) up to 9Hz for the undamped case and up to 3Hz for the damped one, whose peaks quickly diminish. The amplification level is similar to slightly higher for the empirical ratios compared to the theoretical, which is usually the case (Bard, 1999). So the results show good agreement, indicating that the model is satisfactory.

Table 2. The earthquake dataset used for producing the SSR and HVSR empirical ratios.

CORSSA

YEAR	MONTH	DAY	HOUR:	MIN:	SEC	N[°]	E[°]	h [km]	M_L
2002	JUL	28	14	33	45	37.62	22.65	74	4.0
			17	16	31	37.95	20.73	19	4.9
	DEC	2	4	58	56	37.8	21.15	17	5.3
2003	AUG		12	18	15	38.76	20.67	8	5.1
			16	18	3.9	38.76	20.67	9	5.2
	SEP	30	16	46	12	37.97	21.8	10	4.0
2004	MAY	30	6	59	8	37.09	21.5	17	4.6
2005	MAY		8	55	36	38.26	22.73	104	4.4

OTE

YEAR	MONTH	DAY	HOUR:	MIN:	SEC	N[°]	E[°]	h [km]	ML
2002	FEB	24	0	31	18	38.37	21.72	5	3.8
	APR	15	0	14	54	38.43	26.72	24	3.7
2003	JAN	14	8	3	12	41.06	24.51	20	3.4
	FEB	3	2	18	42	38.37	22	15	3.5
		24	13	10	56	37.99	22.05	17	4.1
	APR	3	16	31	26	38.38	21.96	16	3.4
	JUN	1	1	37	18	38	21.83	16	3.8
		12	23	43	60	38.12	21.68	5	4.2

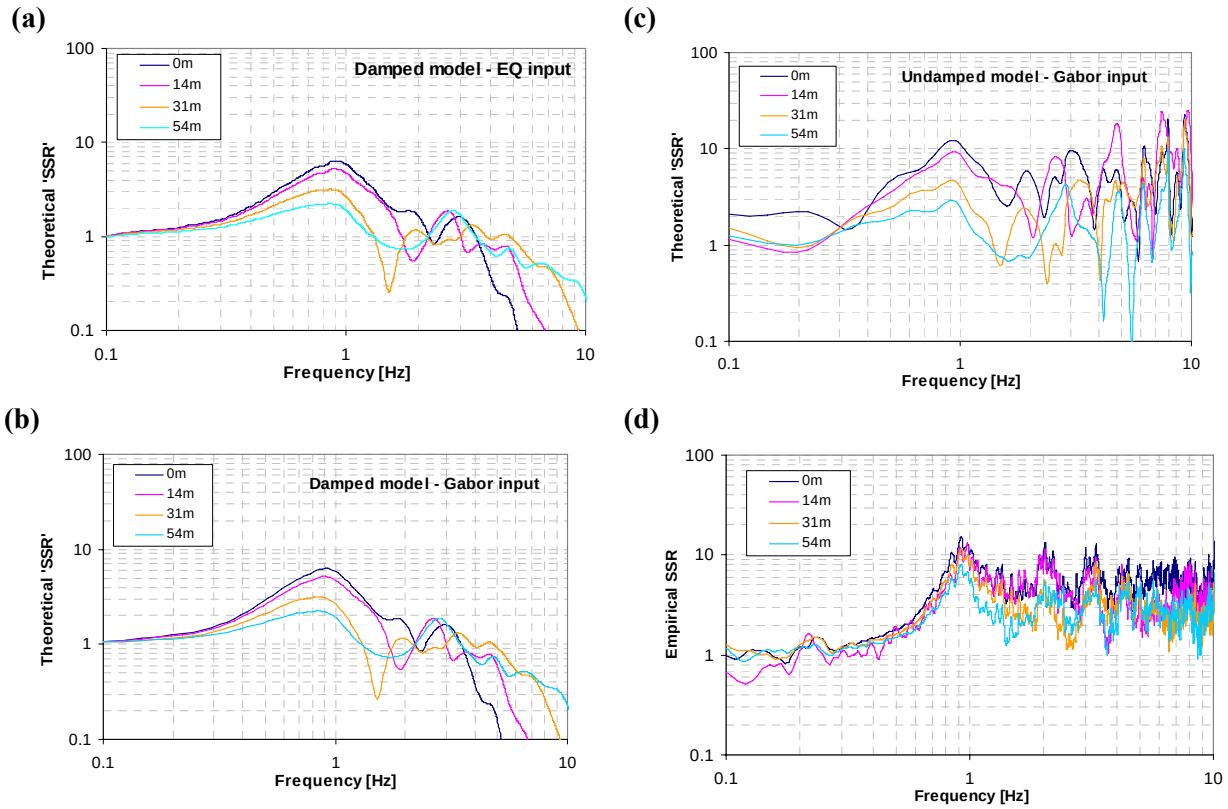

Figure 5. Theoretical 'SSR' for damped model using recording (a) and synthetic input (b) are identical. Theoretical 'SSR' for undamped model (c) closely follows the shape of the empirical SSR (d) up to 9Hz for all four downhole stations of the array (0m, 14m, 31m, 57m).

Surface stations

Horizontal-to-vertical ratios (HVSR) and SSR were estimated based on recordings for the two surface stations available uphill and downhill, pictured in Figure 2 as OTE and CORSSA respectively. The earthquakes used for the OTE station are shown in Table 2 (no simultaneous events at both stations were available). In Figure 6 comparisons are shown with theoretical transfer functions, also including noise HVSR (after Apostolidis et al., 2005) and indicating good agreement around the fundamental (1D) frequencies. However, in the case of OTE the recordings also indicate some shorter frequency peaks around 2-3Hz, compared to the noise and analysis, while in the CORSSA case the SSR amplification is much higher than that of the theoretical, HVSR and noise ratios over higher frequencies.

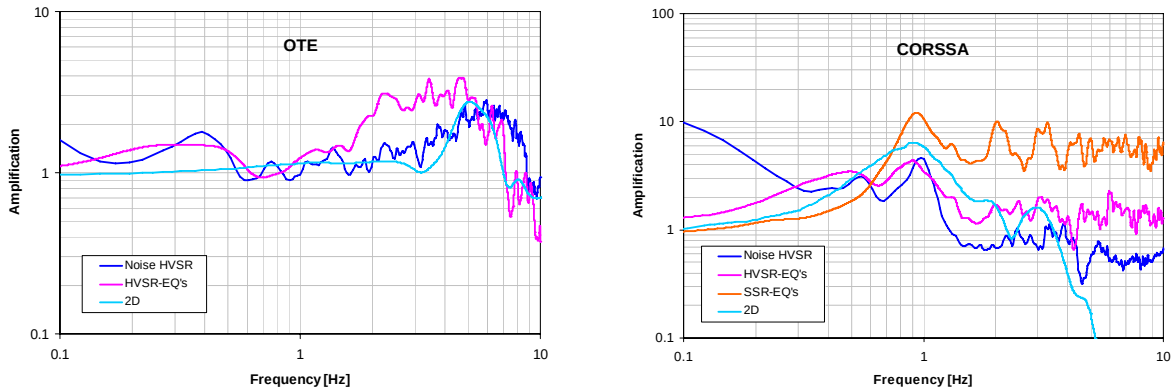

Figure 6. Numerical 2D spectral ratios compared to earthquake SSR and HVSR and to microtremor HVSR ratios at OTE and CORSSA surface stations, indicating good agreement.

Sites along the surface

Theoretical transfer functions were estimated along the surface of the model at 15 sites, uphill and downhill, where noise measurements had already been performed and results were available (Apostolidis et al., 2005). For these transfer functions the resonant frequency was read along with the corresponding amplification factor, and these were plotted along with the values given by the microtremor study. The comparison is shown in Figure 7, where it is seen that the agreement is fairly good uphill. Downhill agreement is good further away but exhibits some discrepancy in frequency near the toe. The amplification factor cannot be expected to coincide anyway, given the doubts expressed by various researchers as to the significance of the amplitude of noise HVSR (Kudo, 1995).

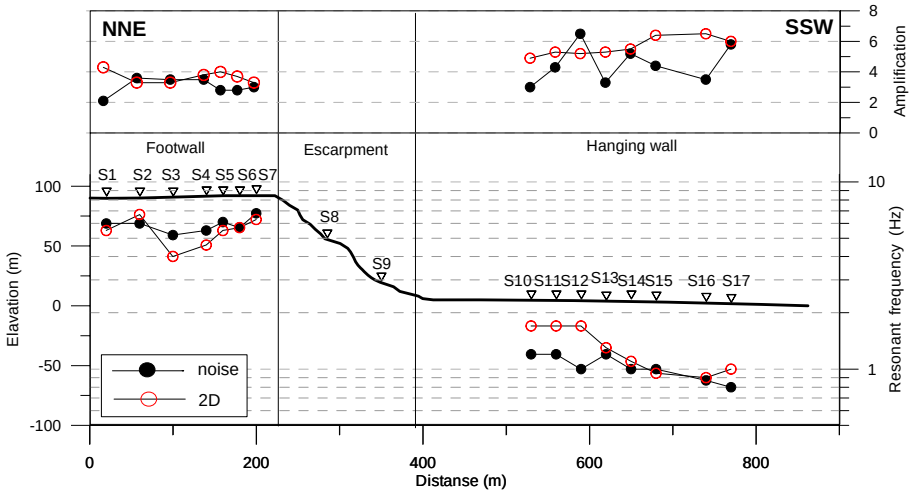

Figure 7. Theoretical transfer functions from 2D numerical analysis and HVSR from noise measurements, in terms of resonant frequency and amplification, at 15 sites along the surface. Good agreement for fundamental frequencies at most locations.

PARAMETRIC ANALYSES

The previous part showed that the initial complex model works well enough when compared to instrumental data from the site, while also revealing the site's complex response. As has already been mentioned, this site consists of several characteristic features which render it complex. So in this part some parametric analyses will attempt to highlight the effects of each of these features, by using different models which include one, some or all of them.

Models investigated

Five models were used, shown in Figure 8:

- the complex actual model used in the previous aprt, including all features uphill and downhill (a)
- a homogeneous conglomerate including only the downhill deposits, grouped into two layers (b)
- a homogeneous conglomerate including only the downhill deposits, grouped into a single layer (c)
- a homogeneous conglomerate containing no soft soils (d)
- a homogeneous conglomerate including only the uphill surface deposit (e)

The soil properties for case (a) are the same as those shown in Table 1. For the new models, the values are the same for the uphill soil deposit and the conglomerate, while in the case of layer grouping a weighted average is used (see Figure 8).

The analysis is performed in the same way as described above, the only difference being that this time the input motion consists solely of Gabor wavelets, since they were proven for the purposes of this study to be just as effective as accelerograms while offering a tremendous advantage in calculation time. Damping is assumed as described in the previous part.

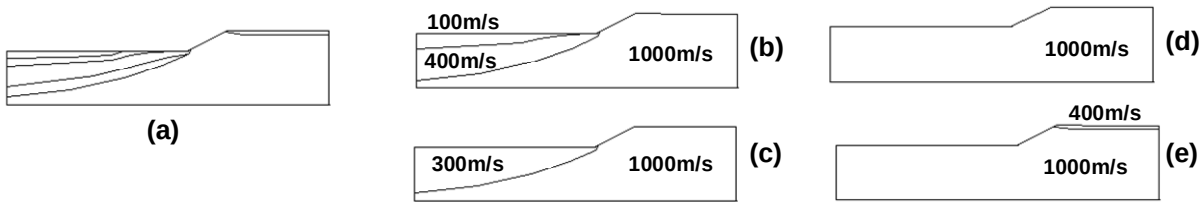

Figure 8. The five models used in the parametric analyses along with the values assumed for Vs.

Time domain results: topographic and basin effects

Representative results in the time domain are presented in Figure 9, where the maximum observed value of absolute acceleration is plotted along the surface of the profile (corresponding to 0.5g input motion). Horizontal motion is shown on the left and vertical on the right. It is noted that only horizontal excitation is exerted at the base, but due to the surface and subsurface discontinuities, interfaces and boundaries, the SV waves are refracted and diffracted, thus generating P and SV body waves as well as surface waves respectively. This explains the presence of the vertical component of 'parasitic' motion in the plots, which is smaller but comparable to the horizontal component.

The purely topographic effect given by the homogeneous model (d) indicates amplification of horizontal motion near the crest with respect to the free field by as much as 40%. This follows the pattern of findings in other topographic effect studies, e.g. Assimaki et al. (2005) found similar time-domain amplifications, around 30%, for similar slope inclinations, around 30°, for input up to PGA=0.3g.

As for the 'basin-edge' effect, there doesn't seem to exist any large difference downhill owing to the different assumptions of the layering, whether it be one, two or four layers (i.e., case c, b or a). So the main impedance contrast causing the phenomena there is apparently due to the basement-deposit interface and not the soil-soil interfaces. This has also been postulated by Apostolidis et al. (2005), who took into account an even deeper structure and concluded that the main interface was the conglomerate surface. As for the fluctuation in maximum acceleration observed downhill for these cases, this may be due to constructive and destructive interference patterns occurring in the open basin between vertically incident body waves and laterally propagating surface waves generated at its edge, namely the soil-conglomerate interface.

In Figure 9a, results of model (e) are compared to the actual (a), the maximum values being equal to those of the actual model uphill. Similarly, in Figure 9b, layered models (b) and (c) exhibit almost identical PGA values along the profile compared to the actual model downhill. Thus, regarding PGA values in both directions, the actual complex model could perhaps be seen a 'superimposition' of the simpler ones into which it is split, namely (e) and (b) or (c), with the specific layering features uphill and downhill influencing the response uphill and downhill respectively.

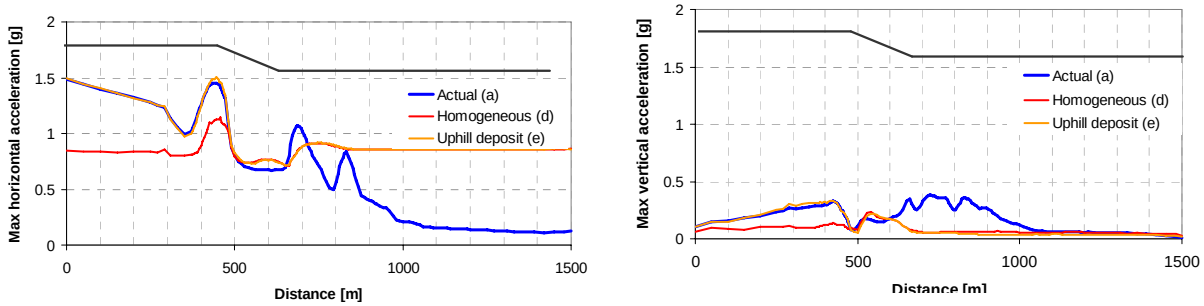

Figure 9a. PGA values along cross-section. Left: horizontal-SV motion, right: vertical-P motion. The actual (a) and homogeneous (d) models are compared with the uphill deposit model (e)

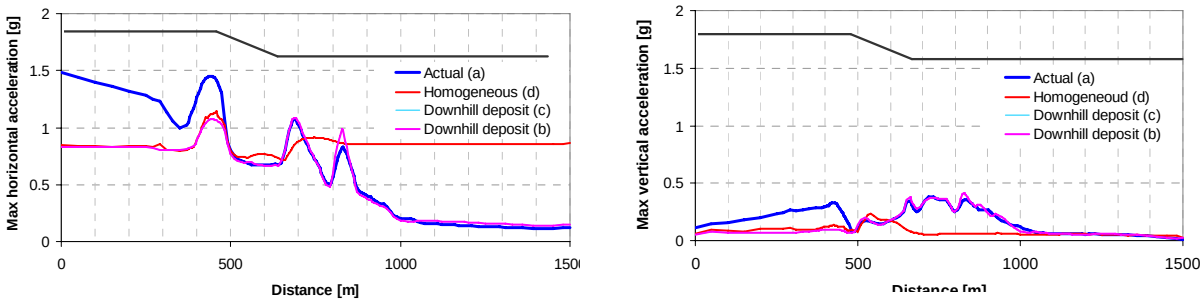

Figure 9b. PGA values along cross-section. Left: horizontal-SV motion, right: vertical-P motion. The actual (a) and homogeneous (d) models are compared with the downhill layered models (b,c).

Figure 10 shows the synthetics derived from the different analyses plotted with time. The horizontal components of motion are presented at the top and the vertical motion time-histories at the bottom. Red traces indicate the crest and toe, encompassing the slope.

For the homogeneous case (d) and, to a lesser degree, for case (e), the first arrivals of the horizontal (SV) motion provide a sketch of the relief, since waves propagate from base to surface at a constant velocity (Vs), or almost. In the other three cases where downhill layering is present (cases a, b, c), this is not the case. The uphill and along-the-slope arrivals do all coincide and thus describe the horizontal relief, but the downhill arrivals are much later (near the far field it takes almost twice the time, due to the smaller Vs values in the deposit basin), indicating a curved line rather than a horizontal one, since the basement-soil interface is curved.

Furthermore, the maximum first-arrival SV amplitude is roughly comparable for the homogeneous and uphill deposit case (cases d, e), while for the downhill deposit cases (a, b, c) due to the high damping the far field motion is nearly five times smaller, making it barely visible. It is noticeable that the maximum amplitudes downhill are clearly not the first SV arrivals, but rather the surface waves generated at the discontinuities of the basin. So these waves are responsible for the high PGA values seen downhill in the previous figure; thus the PGA values seen there do not all correspond to the same wave types or phases. It is worth noting that in similar cases of basin edges, studies have shown that the main phenomenon occurring is 1D resonance and lateral propagation of surface waves generated at the edges through diffraction (Raptakis et al., 2004). In such cases, the surface waves exhibit the same resonant frequency as the incident body waves and only add to the amplification. This can also be related to Figures 5 and 6, where the transfer functions at CORSSA site all showed peaks around 1Hz, which is the 1D fundamental frequency of the soil profile.

It is also visible that all three downhill layered cases (a, b, c) produce very similar waveforms, again indicating that the main factor responsible for these 2D phenomena is the basement-soil rather than the soil-soil interfaces, as seen previously.

Focusing on cases d and e, it can be seen that the topography does not explicitly influence the motion downhill, but produces a fairly strong wavefield uphill, which is enhanced by the surface soil both for the horizontal as well as the vertical component (case e). The surface waves generated by topography are amplified more than the SV arrivals due to the surface soil and clearly seem to propagate much further than the 250m distance from the crest that is plotted in the figure; so the zone influenced in the vicinity of the crest is not a narrow one. The notion that surface soils may accentuate the topographic amplification has been mentioned before, most recently by Assimaki et al. (2005).

Regarding the downhill layered cases a, b, and c, given that the scale is the same, the ‘parasitic’ vertical motion generated downhill is comparable to the horizontal in amplitude. Furthermore, another important ground motion characteristic is duration. These traces clearly indicate that the duration of

ground motion is much longer due to the wave generation and lateral propagation of waves that travel quite far into the thick deposits downhill.

From both Figures 9 and 10, it seems that the phenomena taking place uphill due to the topsoil and relief do not seem to affect the phenomena downhill due to the basin, or vice versa. Nevertheless this is seen as a quite complex case and particularly in the light of the high damping it might be regarded as a 'lower bound' case. Analysis results for a small-strain undamped scenario showed longer wavetrains and larger amplitudes, which may also imply more interference and higher Arias intensities. So for a mildly damped case, the results may be expected to lie somewhere in between the two cases. It can be pointed out here that when material damping is concerned, surface waves are affected more than body waves since the horizontal distance travelled by the former is longer than the vertical distance travelled by the latter. Based on the synthetics, it does not seem impossible that for a steeper slope inclination, interaction might take place between uphill and downhill generated waves. And given the fact that most studies tend to restrict their focus on simplified or even homogeneous models, if this were true then it might be useful to also account for such geomorphological complexities in terms of such 'interaction'.

CONCLUSIONS

The complex site of Aegion is modelled numerically. A 0.5g excitation level is assumed. The code and model sensitivity to type of input and damping are checked through comparisons of the results with instrumental data derived from earthquake recordings as well as microtremor measurements, at surface locations uphill and downhill and at the downhole array. The initial complex model is shown to work well enough, while also revealing the site's complex response.

The site consists of several characteristic features which render it complex. So some parametric analyses are performed on different models with a view to highlighting the effects due to the various geomorphological features: surface topography, surface soil uphill and layered deposits downhill which form a sort of 'basin'. Analyses are performed with synthetic wavelets, proven to be adequate compared to accelerogram input for the scope of this study. The effect of the different factors is illustrated in terms of wavefields and PGA values for both horizontal and 'parasitic' vertical components. Complex wavefields are observed due to diffraction of SV waves and generation and lateral propagation of surface waves downhill at the basin edge. No interaction is clear between phenomena uphill and downhill for this relatively mild slope, rendering the response of the actual case a 'superimposotion' of the responses due to the simpler features comprising it. Long durations are observed, particularly downhill, while the effects there seem to be dictated mainly by the deposit-basement interface. Uphill, topographic effects are visible at distances of a few hundreds of meters from the crest. Due to high damping this could be viewed as a lower bound in motion amplification and wave interference.

AKNOWLEDGEMENTS

The installation of CORSSA was funded by European research project 'CORSEIS' (EVG1-CT-1999-00002) and has been maintained through European projects 'CORSSA' (G1RD-CT-2002-00702) and '3HAZ-CORINTH' (SSPI 004043). The field survey was partially financed by the General Secretariat of Research and Technology, Greece, through Greek project 'XSOILS' (contract DP 23) and European project 'NEMISREF' (G1RD-CT-2002-00702). The financial support of European project 'LESSLOSS' (GOCE-CT-2003-505448) with respect to the numerical analysis is also acknowledged. Prof. K. Makropoulos (National Kapodistrian University of Athens) provided the accelerograms uphill at OTE and D Diagourtas (National Kapodistrian University of Athens) an estimation of distances on the site. The first author wishes to acknowledge financial support through scholarship from the Propondis Foundation and also to thank Prof. F.J. Chavez Garcia (Instituto de Ingeniería, Universidad Nacional Autónoma de México, México D.F. 04510 México) for his fruitful conversation.

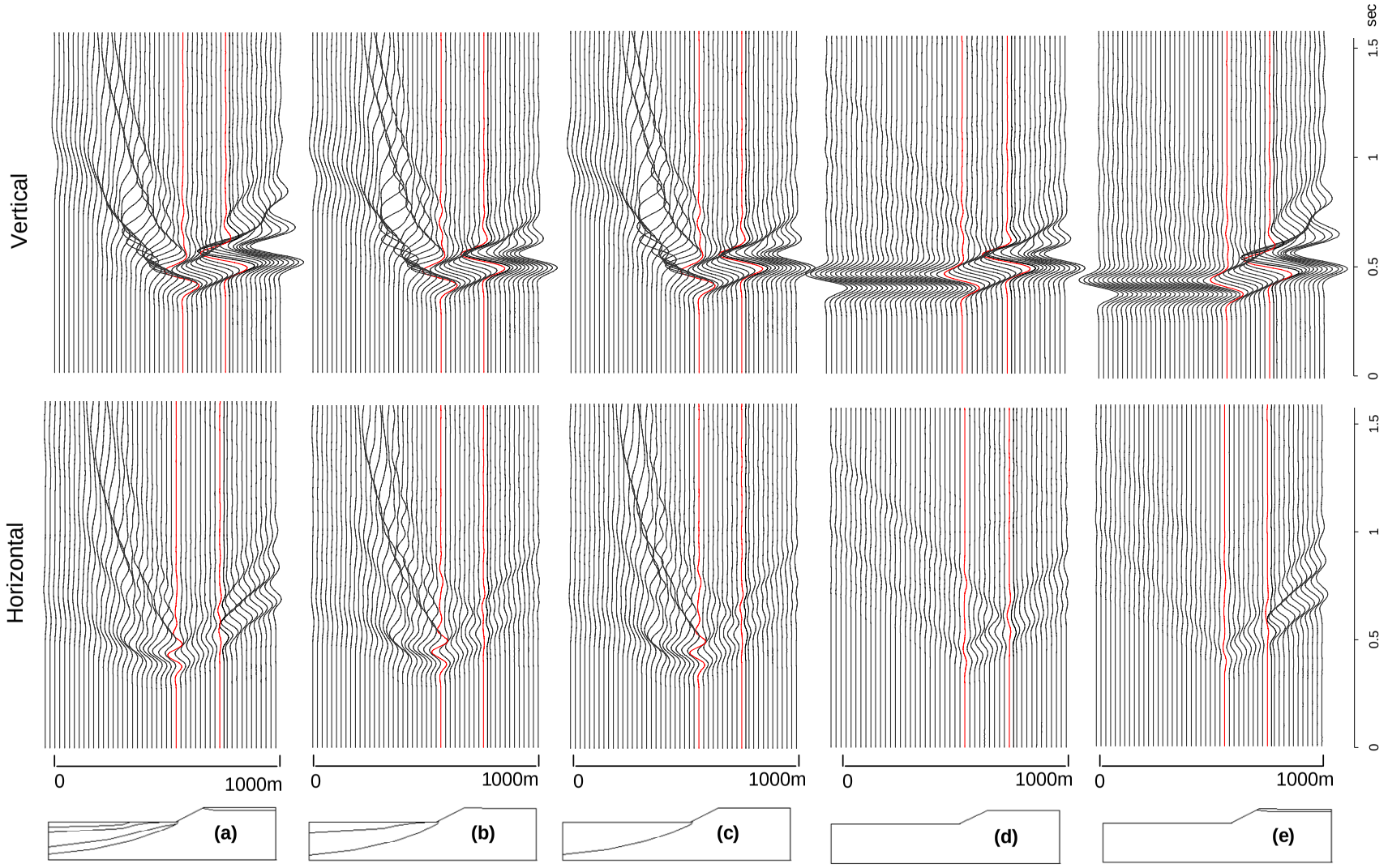

Figure 10. Time histories alonjg cross-section plotted for the 5 damped cases. Top: horizontal motion, bottom: vertical motion.

REFERENCES

Apostolidis, P.,. Raptakis, D, Pandi, K., Manakou, M. and Pitilakis, K. “Definition of subsoil structure and preliminary ground response in Aigion city (Greece) using microtremor and earthquakes”, Soil Dynamics and Earthquake Engineering, Vol. 26, pp. 922 - 940 (2005).

Assimaki D., Kausel E., and Gazetas G. "Soil-dependent topographic effects: A case study from the 1999, Athens Earthquake.". Earthquake Spectra 21.4 (2005): 929-966.

Athanasopoulos G.A., Pelekis P.C., and Leonidou E.A. "Effects of surface topography on seismic ground response in the Egion (Greece) 15 June 1995 earthquake" Soil Dyn. Earth. Eng. 18 (1999): 135-149.

Bard P.-Y. "Local effects on strong ground motion: Physical basis and estimation methods in view of microzoning studies" Proc. of Advanced Study Course in 'Seismotectonic and Microzonation techniques in Earthquake engineering, Kefalonia, Greece (1999).

Bardet, J.P., Ichi, K., Lin, C.H. [2000] EERA: Equivalent-linear Earthquake Site Response Analyses of Layered Soil Deposits. Software Online: http://gees.usc.edu/GEES/Software/EERA2000/Default.htm.

Bouckovalas G.D., and Papadimitriou A.G. "Numerical evaluation of slope topography effects on seimsic ground motion." Soil Dyn. Earthq. Eng. 25.7-8 (2005): 547-558.

Chavez-Garcia F.J., and Faccioli E. "Complex site effects and building codes: Making the leap." J. Seismology 4 (2000): 23-40.

Chavez-Garcia F.J., Rodriguez M., Field E.H., and Hatzfeld D. "Topographic site effects - A comparison of two nonreference methods" Bull. Seism. Soc. Am. 87.6 (1997): 1667-1673.

Chavez-Garcia F.J., Sanchez L.R., and Hatzfeld D. "Topographic site effects and HVSR. A comparison between observations and theory" Bull. Seism. Soc. Am. 86.5 (1996): 1559-1573.

CORSEIS Final Scientific Report, An integrated study of seismic hazard assessment in the area of Aigion, Gulf of Corinth, Greece – EVG1-1999-00002. Laboratory of Soil Mechanics and Foundation, Civil Engineering Department, Aristotle University of Thessaloniki (2002).

Geli L., Bard P.Y., and Jullien B. "The effect of topography on earthquake ground motion: a review and new results." Bull. Seism. Soc. Am. 78.1 (1988): 42-63.

Institute of Geodynamics - NOA: http://www.gein.noa.gr/services/cat.html

ITASCA Consultants FLAC (Fast Lagrangian Analysis of Continua), S. A. Version 4.0. (2002)

Ktenidou O.-J. "2-D dynamic ground response analysis and study of topographic and site effects of strong ground motion for the city of Aegion, Greece" Diploma thesis, Aristotle University of Thessaloniki, Greece (in Greek) (2003).

Kudo K., Practical estimates of site response, State of the art report, in: Proc. of the 5th intern. conf. on seismic zonation, Nice, Ouest editions Nantes, 3, pp 1878-1907, 1995

National Observatory of Athens, Institute of Geodynamics: http://www.gein.noa.gr/services/cat.html

Pitilakis, K., Ktenidou, O.-J., Raptakis, D., Apostolidis, P., Manakou, M., Makropoulos, K. and Diagourtas, D. “Experimental and theoretical study of topographic effects” Proc. 15th International Conference in Soil Mechanics and Geotechnical Engineering: Satellite Conference on Recent Developments in Earthquake Geotechnical Engineering, Osaka, Japan. (2005).

Pitilakis K., Makropoulos K., Bernard P., Lemeille F., Berge-Thierry C., Tika Th., Manakou M., Diagourtas D., Kallioglou P., Makra K., Pitilakis D., and Bonilla L.F. "The Corinth Gulf Soft Soil Array (CORSSA) to study site effects" Comptes Rendus Geoscience 336.4-5 (2004): 353-365.

Pitilakis K., Raptakis D., Makra K., Ktenidou O.-J., Pandi K., Manakou M., Pitilakis D., and Diagourtas D. "Effects of surface and subsurface topography on strong ground motion at the city of Aegion-Greece" 13th World Conf. Earth. Eng. Vancouver, BC, Canada (2004b).

Raptakis D., Makra K., Anastasiadis A., and Pitilakis K. "Complex site effects in Thessaloniki (Greece): II. 2D SH modelling and engineering insights." Bull. Earthq. Eng. 2 (2004): 301-327.

Sanchez-Sesma F.J., and Campillo M. "Topographic effects for incident P, SV and Rayleigh waves." Tectonophysics 218 (1993): 113-125.